

Effect of temperature on tensile properties of hot rolled AZ31 Mg alloy sheets

J. Balík¹, P. Lukáč^{1*}, J. Bohlen², K. U. Kainer²

¹*Department of Physics of Materials, Charles University, Ke Karlovu 5, 121 16 Prague, Czech Republic*

²*GKSS Research Centre Geesthacht, Max-Planck-Straße 1, 215 02 Geesthacht-Tesperhude, Germany*

Received 2 April 2007, received in revised form 30 April 2007, accepted 30 April 2007

Abstract

Mechanical properties of AZ31 H24 magnesium alloy sheets were investigated by tensile tests over a wide temperature range from room temperature to 400 °C at an initial strain rate of $1.3 \times 10^{-3} \text{ s}^{-1}$. The deformation behaviour of the AZ31 alloy sheet was also investigated after annealing. The yield stress and the maximum stress decrease with increasing temperature. The values of the yield stress and maximum stress of the samples with tensile axis parallel to the rolling direction are lower than those of the samples deformed perpendicular to the rolling direction. The elongation to failure increases very rapidly with increasing temperature. The results are explained by the dislocation glide in the basal and non-basal slip systems and by deformation twinning.

Key words: magnesium alloy, mechanical properties, dislocation mechanisms

1. Introduction

Investigations of the deformation behaviour of commercial cast magnesium alloys have shown that their elongation to failure, if deformed at room temperature, is low, in most cases only a few percent. The elongation to failure may increase with increasing temperature reaching about 30 % at 300 °C [1]. Limited ductility of Mg alloys may be due to their hexagonal close packed structure. According to the Taylor criterion [2], five independent slip systems are required for homogeneous deformation of polycrystalline materials. The dominant slip mode for the hexagonal crystals such as Mg at ambient temperature is the basal slip. The number of independent mode for the basal slip is only two, which is not sufficient for the satisfying the Taylor criterion [2]. The activity of non-basal slip systems is therefore required. In Mg, the glide of dislocations in second-order pyramidal slip systems should be considered [3, 4]. For magnesium and its alloys, the critical resolved shear stresses of non-basal slip systems are much higher than for the basal slip system at room temperature [5–10]. On the other hand, the critical resolved shear stresses for non-basal slip

systems decrease very rapidly with increasing temperature. Thus, the activity of dislocation slip in the non-basal systems increases with increasing temperature, which should result in a higher ductility of Mg alloys with increasing temperature. The deformation behaviour of Mg alloys depends also on alloying elements; see e.g. [11–14]. Dynamic strain ageing associated with solute atoms is observed in some magnesium alloys, if deformed at certain temperatures [15–17].

Magnesium wrought alloys with improved mechanical properties may find high engineering applications. Some structure products are made from fine-grained sheets using superplastic gas pressure forming. In our last papers [18, 19] we could show that the mechanical properties of AZ31 magnesium alloy sheets are strongly influenced by the test temperature. The commercial AZ31 alloy was investigated over a wide temperature range from room temperature to 400 °C. The yield stress and maximum stress decrease with increasing temperature and the strain to fracture increases with increasing temperature. A preheating temperature may influence the yield stress and the maximum stress of AZ31 magnesium alloys prepared by hot rolling [20]. The texture and the microstruc-

*Corresponding author: tel.: +420 221911366; fax: +420 221911490; e-mail address: lukac@met.mff.cuni.cz

ture of rolled AZ31 sheets in the stress-relieved (H24) temper are also influenced by annealing [21].

The aim of the present work is to study the influence of temperature on the tensile behaviour of AZ31 Mg alloy sheets, with the tensile axes parallel and perpendicular to the rolling direction, at temperatures between room temperature and 400 °C. The differences between the mechanical response of both the rolled H24 structure and the pre-aged one are focused as well.

2. Experimental procedure

Commercial magnesium alloy AZ31 (the nominal chemical composition: Mg-3Al-0.9Zn-0.15Mn in mass %) sheets in stress-relieved (H24) state were studied in the present work. The average grain size after rolling was $45 \pm 5 \mu\text{m}$. The rolled sheets had basal texture – in most cases, grains are oriented such that their (0001) basal planes are close to the plane of the sheet and the $\langle 11\bar{2}0 \rangle$ direction was very close to the rolling direction. Tensile specimens of 25 mm gauge length, 5 mm width and with a thickness of 1.6 mm were machined. Tensile tests were carried out at a constant cross head speed using an INSTRON universal testing machine. The tests were conducted between room temperature and 400 °C at an initial strain rate of $1.3 \times 10^{-3} \text{ s}^{-1}$. The temperature was controlled to within $\pm 2^\circ\text{C}$. The tensile axis was chosen parallel or perpendicular to the rolling direction.

Some sheets were annealed in a furnace at different temperatures and Vickers microhardness (HV_m) was measured, after annealing, on the polished surfaces under a load of 100 g for 15 s. Each data point was the mean value of at least ten indentations. Microstructural features were examined by light microscopy (Olympus IX 70). Metallographic specimens were cut from the sheets, mechanically ground on progressively finer grade of SiC impregnated paper and then mechanically polished. Specimens were etched in a solution 5 ml acetic acid, 6 g picric acid, 100 ml ethanol and 10 ml H₂O.

3. Experimental results

The variation of microhardness as a function of the annealing temperature and time is shown in Fig. 1. After an initial drop over the period of 2 h, microhardness is practically stabilised, whereas the grain size is gradually increasing.

The microstructure of magnesium alloy AZ31 sheets was investigated in detail in [22, 23]. A typical microstructure of the as-received specimens is shown in Fig. 2. The microstructural observations revealed inhomogeneous grain size distribution. Twins

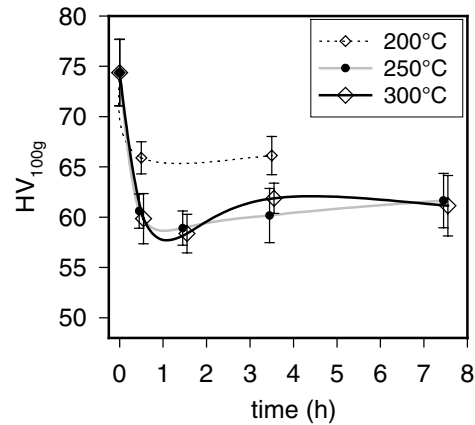


Fig. 1. Ageing curves for microhardness.

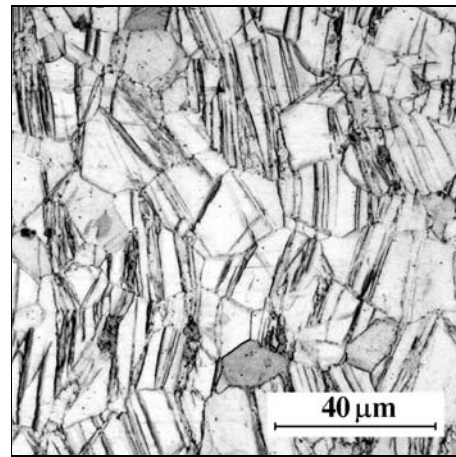


Fig. 2. Initial state H24, rolling direction horizontal.

are present in many grains. They are often either perpendicular or deviated to the rolling direction [19]. Changes in the microstructure after annealing are illustrated in Fig. 3. Annealing results in a more homogeneous microstructure. The volume fraction of twins observed in the light microscope decreases with increasing annealing temperature. Most of twins are eliminated.

The true stress-true strain curves of the AZ31 specimens in H24 condition (hereafter H24) with the tensile axis parallel to the rolling direction obtained at various temperatures are shown in Fig. 4. It can be seen that the flow stress decreases and the elongation to fracture increases with increasing testing temperature. Two flow curves at 100 and 200 °C presented in Fig. 4 show small scatters in ductilities. At higher temperatures, above 250 °C, the flow stress is practically independent of strain; no significant work hardening was observed for any specimens. The results indicate that dynamic recovery can take place. The values

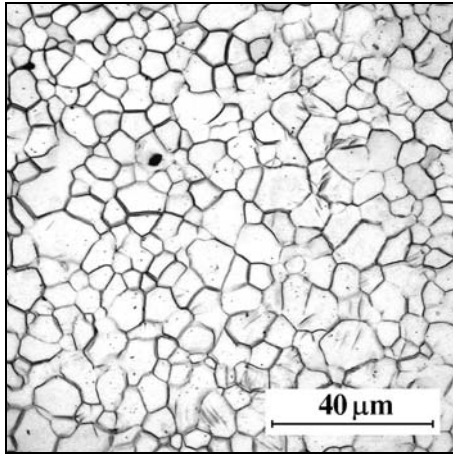


Fig. 3. State after ageing for 7.5 h at 300°C. Mean intercept $\lambda = 8.6 \mu\text{m}$, grain size $d = 1.7$, $\lambda = 14.9 \mu\text{m}$.

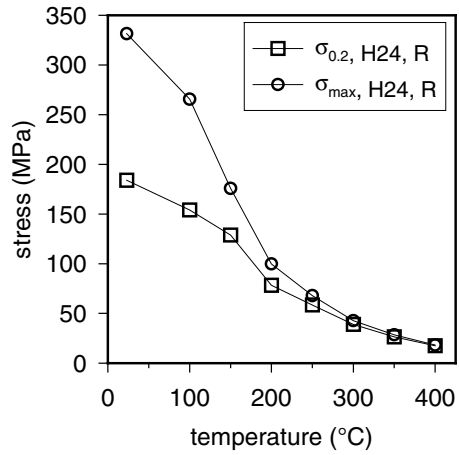


Fig. 5. Yield and maximum stresses for initial state H24 and tensile axis R.

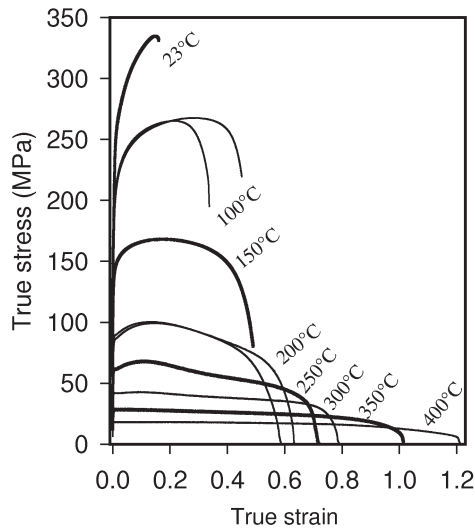


Fig. 4. Tensile curves for initial state H24 and tensile axis R.

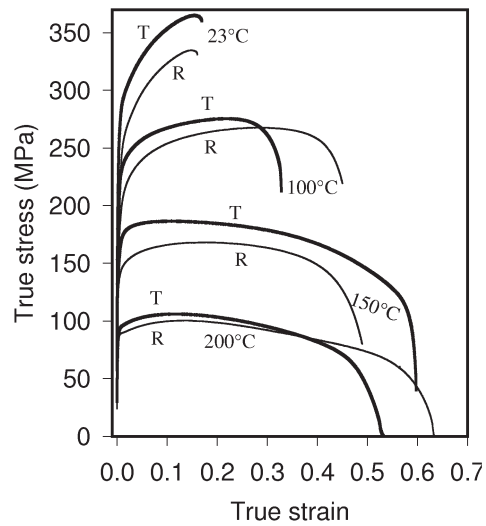


Fig. 6. Tensile curves for initial state H24, comparison of tensile axes R and T.

of the yield stress, $\sigma_{0.2}$, determined as the flow stress at 0.2 offset strain and the maximum stress, σ_{max} , determined as the maximum flow stress are plotted against temperature in Fig. 5. Figure 5 shows that both $\sigma_{0.2}$ and σ_{max} decrease very rapidly with increasing temperature. The values of $\sigma_{0.2}$ and σ_{max} are practically the same at and above 250°C, which corresponds to nonsignificant work hardening identified by a nearly constant flow stress.

To estimate the effect of loading orientation on tensile properties, two types of specimens: a) specimens with tensile axis parallel to the rolling direction (hereafter R specimens) and b) specimens with tensile axis perpendicular to the rolling direction (transversal direction, hereafter T specimens) were tested. Figure 6 shows representative true stress-true strain curves

for both specimen types. It is obvious that there is a difference in the flow stress. The flow stresses of T specimens are higher than those of R specimens. On the other hand, at a temperature of 200°C, the flow curves for both specimen types are very similar.

Figure 7 shows the true stress-true strain curves for the sheets deformed after annealing (at 300°C/8 h) at an initial strain rate of $1.3 \times 10^{-3} \text{ s}^{-1}$ at different temperatures ranging from room temperature to 250°C. The specimens were deformed with tensile axis parallel to the rolling direction. It can be seen that the influence of temperature on the course of the stress-strain curves is qualitatively the same as for the as-received specimens. For comparison, the flow curves for both annealed (A) specimens and the specimens in the H24 condition (H) are given in Fig. 7.

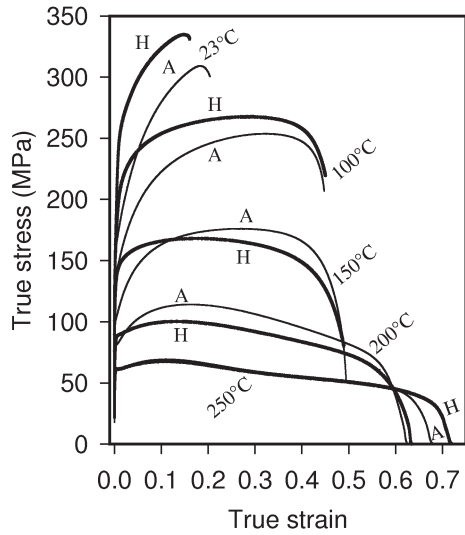


Fig. 7. Comparison of tensile curves for aged state 300°C/8 h (A) and initial state H24 (H). Tensile axis R.

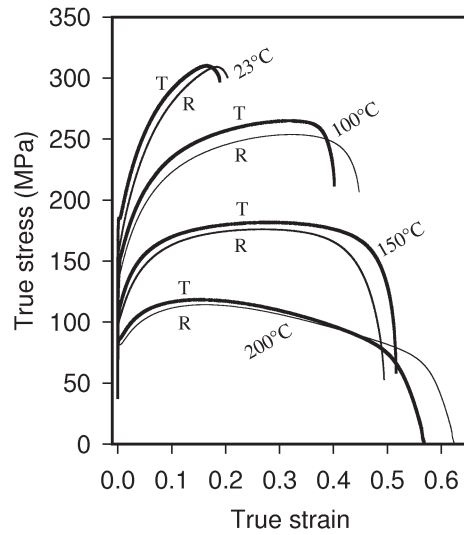


Fig. 9. Tensile curves for aged state 300°C/8 h, comparison for tensile axes R and T.

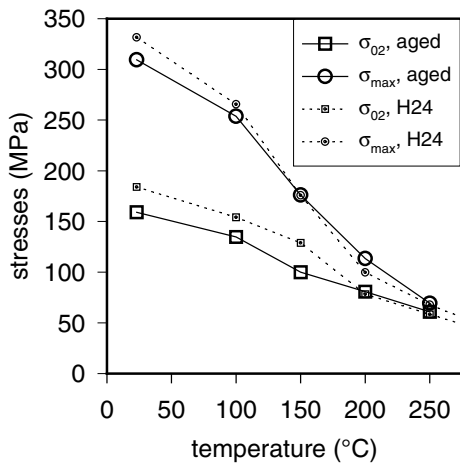


Fig. 8. Yield and maximum stresses for aged state 300°C/8 h and tensile axis R.

The flow stresses at 23 and 100°C are lower for the annealed sheets, whereas the flow stress for A specimens is higher than that for H specimens deformed at 200°C. Note the flow curves at 150°C – the flow stress for the A specimens at the beginning deformation (low strains) is lower than for the H specimens, whereas the flow stress for the A specimens at higher strains is higher than for the H specimens. A steady state – deformation at a constant flow stress – is obtained at a temperature of 250°C. At this temperature, the flow curves for both specimen types are practically the same. Figure 8 shows the temperature variations of the yield stress, σ_{02} , and the maximum stress, σ_{max} , for the annealed structure in comparison to the initial H24 state. The effect of annealing on the yield stress

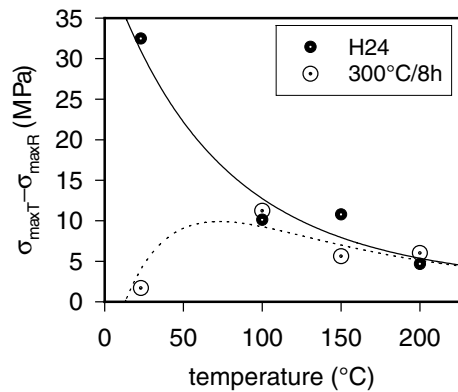


Fig. 10. Plastic anisotropy in terms of maximum stresses for both initial state H24 and aged state 300°C/8 h.

is significant at the testing temperatures below 200°C.

Figure 9 shows the effect of the tensile direction with respect to the rolling direction on the deformation behaviour of the annealed specimens at different testing temperature over a temperature range from room temperature to 200°C. The flow stress of the specimens with tensile axis perpendicular to the rolling direction (T specimens) is higher than that for the specimens deformed parallel to the rolling direction (R specimens) – the anisotropy is observed. The flow stress for both deformation modes decreases with increasing temperature. The anisotropy characteristics – defined as the difference between the maximum stress of specimens deformed perpendicular to the rolling direction, σ_{maxT} , and the maximum stress of specimens deformed parallel to the rolling direction, σ_{maxR} , i.e. $\sigma_{maxT} - \sigma_{maxR}$, are plotted against the testing tem-

perature in Fig. 10. The anisotropy characteristics are shown for both structure types.

4. Discussion

The flow curves in Figs. 4, 6, 7, and 9 show changes in the shape of the stress-strain curves with the testing temperatures. The shape of the flow curves is influenced not only by the testing temperature but also by heat treatment. The deformation behaviour is also influenced by the tensile direction with the respect to the rolling direction, especially at low temperatures (Figs. 6, 9 and 10). At temperatures above 250 °C, the work hardening rate is very close to zero. Such a steady-state deformation occurring at higher temperatures may be a result of a dynamic balance between hardening and softening processes, including processes related to dynamic recovery. The processes of softening are thermally activated ones. From the dislocation theory point of view, it means that there is a dynamic balance between storage of dislocations leading to hardening and annihilation of dislocations leading to softening. The intensity of the latter is highly dependent on temperature. The activity of non-basal slip systems plays an important role in both hardening and recovery processes in magnesium alloys.

From the activities of the non-basal slip modes, motion of dislocations with $\langle c + a \rangle$ Burgers vector in the second-order pyramidal slip systems is expected [3, 24–28]. The Taylor [2] criterion is then fulfilled resulting in further straining and enhanced ductility. Moreover, the glide of $\langle c + a \rangle$ dislocations may be responsible for an additional work hardening because of the development of several systems of immobile or sessile dislocations. Different reactions between $\langle a \rangle$ basal dislocations and $\langle c + a \rangle$ pyramidal dislocations can occur [3, 24, 27]. Within the basal plane, immobile $\langle c \rangle$ dislocations may arise by the following reactions:

$$\frac{1}{3} \langle 2\bar{1}\bar{1}3 \rangle_{gl} \rightarrow \langle 0001 \rangle + \frac{1}{3} \langle 2\bar{1}\bar{1}0 \rangle$$

or

$$\frac{1}{3} \langle 2\bar{1}\bar{1}3 \rangle_{gl} + \frac{1}{3} \langle 2\bar{1}10 \rangle \rightarrow \langle 0001 \rangle,$$

where the subscript gl denotes glissile (glide) dislocation. Another reaction that employs the basal $\langle a \rangle$ dislocation yields a sessile $\langle c + a \rangle$ dislocation (subscript ses)

$$\frac{1}{3} \langle 2\bar{1}\bar{1}3 \rangle_{gl} + \frac{1}{3} \langle \bar{1}2\bar{1}0 \rangle \rightarrow \frac{1}{3} \langle 11\bar{2}3 \rangle_{ses}.$$

Finally, a combination of two glissile $\langle c + a \rangle$ dislocations gives rise to a sessile dislocation of $\langle a \rangle$ type,

which lays along the intersection of the second order pyramidal planes, according to the reaction

$$\frac{1}{3} \langle 2\bar{1}\bar{1}3 \rangle + \frac{1}{3} \langle \bar{1}2\bar{1}3 \rangle \rightarrow \frac{1}{3} \langle 11\bar{2}0 \rangle_{ses}.$$

Dislocation reactions may produce sessile dislocations and an increase in the density of the forest dislocations. In both cases, additional obstacles of the dislocation type are formed and hence an increase in hardening should result. On the other hand, screw dislocations of the $\langle c + a \rangle$ type can move to the parallel slip planes by double cross slip. Then, annihilation of dislocations can follow, the dislocation density decreases and softening occurs, which causes a decrease in the work hardening rate. It is obvious that the softening processes depend strongly on the testing temperature. The glide of $\langle c + a \rangle$ dislocations depends on the testing temperature, applied stress and microstructure (the densities of basal and pyramidal dislocations). The activation of non-basal slip system depends on the testing temperature – the critical resolved shear stress for pyramidal slip system rapidly decreases as the temperature is increased. At lower temperatures, grain boundaries and twins act as obstacles to dislocation motion, which results in dislocation pile-ups. The stress concentration at the head of pile-ups may initiate the activity of the pyramidal slip system – the $\langle c + a \rangle$ dislocations may move. A possible source mechanism for non-basal $\langle c + a \rangle$ dislocations as proposed by Yoo et al. [29] cannot be excluded.

The observed anisotropy at temperatures below about 150 °C, i.e. the strength of T specimens is higher than that of R specimens, is connected with the texture. On the contrary, the nearly isotropy at temperatures above 150 °C may be a consequence of the enhanced activity of the pyramidal slip systems. The critical resolved shear stress (CRSS) for the pyramidal slip system decreases very rapidly with temperature. As the temperature rises, the CRSS ratio between non-basal $\langle c + a \rangle$ slip and basal slip decreases, which makes easy the glide and cross slip of $\langle c + a \rangle$ dislocations. This behaviour is in agreement with plastic anisotropy simulation by Agnew and Dyugulu [30].

The increase in the strain to fracture connecting with a decrease in the flow stress may be also explained by an increase in the activity of non-basal slip systems with increasing temperature.

5. Conclusions

The work hardening behaviour of an AZ31 magnesium alloy was investigated at several temperatures between room temperature and 400 °C at strain rate of $1.3 \times 10^{-3} \text{ s}^{-1}$. The test temperature influences significantly the deformation behaviour of the

alloy. The deformation behaviour is influenced by heat treatment. The yield stress and the maximum flow stress decrease very rapidly with increasing temperature from about 180 MPa at room temperature to about 10 MPa at 400 °C for the yield stress and from about 340 MPa to about 10 MPa at 400 °C for the maximum stress. The work hardening rate decreases with increasing temperature; it becomes very close to zero at higher temperatures. The deformation behaviour of the AZ31 sheets at different temperatures can be attributed to the activity of non-basal slip systems. Dislocation glide on the second order pyramidal planes and double cross slip of $\langle c + a \rangle$ dislocations have a significant effect on the deformation behaviour, especially at elevated temperatures.

Acknowledgements

We would like to dedicate this paper to Prof. Dr. Zuzanka Trojanová, DrSc., at the occasion of her 65th birthday. This work was financed by the Ministry of Education of the Czech Republic under the Research Project 1M2560471601 Eco-centre for Applied Research of Non-ferrous Metals. P. L. is grateful for the support offered by the Grant Agency of the Academy of Sciences of the Czech Republic under grant A201120603. The authors thank Dr. Aleš Jäger for supplying Figure 2 and some data used in Figures 4 and 5.

References

- [1] ASM Specialty Handbook Magnesium and Magnesium Alloys. Eds.: Avedesian, M. M., Baker, H. Materials Park, OH, ASM International 1999.
- [2] TAYLOR, G. I.: *J. Inst. Met.*, 62, 1938, p. 307.
- [3] LUKÁČ, P.: *Czech. J. Phys. B*, 31, 1981, p. 135.
- [4] AGNEW, S. R.—HORTON, J. A.—YOO, M. H.: *Metall. Mater. Trans. A*, 33, 2002, p. 851.
- [5] YOSHINAGA, H.—HORIUCHI, R.: *Trans JIM*, 5, 1963, p. 14.
- [6] URAKAMI, A.—MESHI, M.—FINE, M. E.: In: *Proceedings ICSMA 2*, Vol. 1, Asilomar, ASM 1970, p. 272.
- [7] AKHTAR, A.—TEGHTSOONIAN, E.: *Acta Metall.*, 17, 1969, p. 1351.
- [8] STOHR, J. F.—POIRIER, J. P.: *Phil. Mag.*, 25, 1972, p. 1313.
- [9] ANDO, S.—NAKAMURA, K.—TAKASHIMA, K.—TONDA, H.: *J. Japan Inst. Light Metals*, 42, 1992, p. 765.
- [10] ANDO, S.—TONDA, H.: *Mater. Sci. Forum*, 350-351, 2000, p. 43.
- [11] CÁCERES, C. H.—ROVERA, D. M.: *J. Light Metals*, 1, 2001, p. 152.
- [12] CÁCERES, C. H.—BLAKE, A.: *Phys. Stat. Sol. (a)*, 194, 2002, p. 147.
- [13] MÁTHIS, K.—TROJANOVÁ, Z.: *Kovove Mater.*, 43, 2005, p. 238.
- [14] TROJANOVÁ, Z.—MILNERA, M.: *Kovove Mater.*, 44, 2006, p. 75.
- [15] TROJANOVÁ, Z.—LUKÁČ, P.: *Kovove Mater.*, 43, 2005, p. 73.
- [16] TROJANOVÁ, Z.—LUKÁČ, P.—KAINER, K. U.: *Adv. Eng. Mater.*, 7, 2005, p. 1027.
- [17] LUKÁČ, P.—TROJANOVÁ, Z.: In: *Magnesium*. Ed.: Kainer, K. U. Weinheim, WILEY-VCH 2007, p. 575.
- [18] JÄGER, A.—LUKÁČ, P.—GÄRTNEROVÁ, V.—BOHLEN, J.—KAINER, K. U.: *J. Alloy Comp.*, 378, 2004, p. 184.
- [19] JÄGER, A.—LUKÁČ, P.—GÄRTNEROVÁ, V.: *Kovove Mater.*, 42, 2004, p. 165.
- [20] JANEČEK, M.—ŠUPÍK, V.—HOLLÄNDER, F.—WENDT, J.: *Kovove Mater.*, 43, 2005, p. 218.
- [21] JÄGER, A.—LUKÁČ, P.—GÄRTNEROVÁ, V.—HALODA, J.—DOPITA, M.: *Mater. Sci. Eng. A*, 432, 2006, p. 20.
- [22] KAISER, F.—LETZIG, D.—BOHLEN, J.—STYCZYNSKI, A.—HARTIG, C.—KAINER, K. U.: *Mater. Sci. Forum*, 419-422, 2003, p. 315.
- [23] BOHLEN, J.—HORTSMANN, A.—KAISER, F.—STYCZYNSKI, A.—LETZIG, D.—KAINER, K. U.: In: *Magnesium Technology 2003*. Ed.: Kaplan, H. J. Warrendale, PA, TMS 2003, p. 253.
- [24] LUKÁČ, P.: *Czech. J. Phys. B*, 35, 1985, p. 275.
- [25] AGNEW, S. R.—YOO, M. H.—TOMÉ, C. N.: *Acta Mater.*, 49, 2001, p. 4077.
- [26] MÁTHIS, K.—NYILAS, K.—AXT, A.—DRAGOMIR-CERNATESCU, I.—UNGÁR, T.—LUKÁČ, P.: *Acta Mater.*, 52, 2004, p. 2889.
- [27] LUKÁČ, P.—MÁTHIS, K.: *Kovove Mater.*, 40, 2002, p. 281.
- [28] KOIKE, J.—KOBAYASHI, T.—MUKAI, T.—WATANEBE, H.—SUZUKI, M.—MARUYAMA, K.—HIGASI, K.: *Acta Mater.*, 51, 2003, p. 2055.
- [29] YOO, M. H.—AGNEW, S. R.—MORRIS, J. R.—HO, K. M.: *Mater. Sci. Eng. A*, 321, 2001, p. 87.
- [30] AGNEW, S. R.—DUYGULU, O.: *Inter. J. Plasticity*, 21, 2005, p. 1161.